



# Growth Mode and Carbon Source Impact the Surfaceome Dynamics of *Lactobacillus rhamnosus* GG

Kirsi Savijoki<sup>1,2</sup>, Tuula A. Nyman<sup>3</sup>, Veera Kainulainen<sup>4</sup>, Ilkka Miettinen<sup>2</sup>, Pia Siljamäki<sup>1</sup>, Adyary Fallarero<sup>2</sup>, Jouko Sandholm<sup>5</sup>, Reetta Satokari<sup>4</sup> and Pekka Varmanen<sup>1\*</sup>

<sup>1</sup> Department of Food and Nutrition, University of Helsinki, Helsinki, Finland, <sup>2</sup> Division of Pharmaceutical Biosciences, University of Helsinki, Helsinki, Finland, <sup>3</sup> Department of Immunology, Institute of Clinical Medicine, University of Oslo and Oslo University Hospital, Oslo, Norway, <sup>4</sup> Human Microbiome Research Program, Faculty of Medicine, University of Helsinki, Helsinki, Finland, <sup>5</sup> Turku Bioscience, University of Turku and Åbo Akademi University, Turku, Finland

## OPEN ACCESS

### Edited by:

Rosa Anna Siciliano,  
Italian National Research Council  
(CNR), Italy

### Reviewed by:

Silvina Graciela FADDA,  
CONICET Centro de Referencia para  
Lactobacilos (CERELA), Argentina  
Clifton Fagerquist,  
United States Department  
of Agriculture, United States

### \*Correspondence:

Pekka Varmanen  
pekka.varmanen@helsinki.fi

### Specialty section:

This article was submitted to  
Food Microbiology,  
a section of the journal  
Frontiers in Microbiology

**Received:** 15 March 2019

**Accepted:** 22 May 2019

**Published:** 05 June 2019

### Citation:

Savijoki K, Nyman TA,  
Kainulainen V, Miettinen I, Siljamäki P,  
Fallarero A, Sandholm J, Satokari R  
and Varmanen P (2019) Growth Mode  
and Carbon Source Impact  
the Surfaceome Dynamics  
of *Lactobacillus rhamnosus* GG.  
Front. Microbiol. 10:1272.  
doi: 10.3389/fmicb.2019.01272

Bacterial biofilms have clear implications in disease and in food applications involving probiotics. Here, we show that switching the carbohydrate source from glucose to fructose increased the biofilm formation and the total surface-antigenicity of a well-known probiotic, *Lactobacillus rhamnosus* GG. Surfaceomes (all cell surface-associated proteins) of GG cells grown with glucose and fructose in planktonic and biofilm cultures were identified and compared, which indicated carbohydrate source-dependent variations, especially during biofilm growth. The most distinctive differences under these conditions were detected with several surface adhesins (e.g., MBF, SpaC pilus protein and penicillin-binding proteins), enzymes (glycoside hydrolases, PrsA, PrtP, PrtR, and HtrA) and moonlighting proteins (glycolytic, transcription/translation and stress-associated proteins, r-proteins, tRNA synthetases, Clp family proteins, PepC, PepN, and PepA). The abundance of several known adhesins and candidate moonlighters, including enzymes acting on casein-derived peptides (ClpP, PepC, and PepN), increased in the biofilm cells grown on fructose, from which the surface-associated aminopeptidase activity mediated by PepC and PepN was further confirmed by an enzymatic assay. The mucus binding factor (MBF) was found most abundant in fructose grown biofilm cells whereas SpaC adhesin was identified specifically from planktonic cells growing on fructose. An additional indirect ELISA indicated both growth mode- and carbohydrate-dependent differences in abundance of SpaC, whereas the overall adherence of GG assessed with porcine mucus indicated that the carbon source and the growth mode affected mucus adhesion. The adherence of GG cells to mucus was almost completely inhibited by anti-SpaC antibodies regardless of growth mode and/or carbohydrate source, indicating the key role of the SpaCBA pilus in adherence under the tested conditions. Altogether, our results suggest that carbon source and growth mode coordinate mechanisms shaping the proteinaceous composition of GG cell surface, which potentially contributes to resistance, nutrient acquisition and cell-cell interactions under different conditions. In conclusion, the present study shows that different growth regimes and conditions can have a profound impact on the adherent and antigenic features of GG, thereby providing new information on how to gain additional benefits from this probiotic.

**Keywords:** *Lactobacillus rhamnosus*, probiotic, biofilm, surface protein, fructose, mucus, adhesion

## INTRODUCTION

Probiotic bacteria, applied in various aspects of the food and pharmaceutical industries (Sanders et al., 2013; Goldenberg et al., 2017), exploit sophisticated strategies to enable the utilization of many nutrients, maintain viability and adherence to mucosal surfaces, and modulate host immunity in a beneficial way during industrial processes and upon their consumption (Siezen and Wilson, 2010). Unlike free-living cells, the biofilm mode of growth has been shown to improve existing probiotic features (antimicrobial and anti-inflammatory functions) in some *Lactobacillus* strains (Jones and Versalovic, 2009; Rieu et al., 2014; Aoudia et al., 2016). In addition, switching from the planktonic to the biofilm mode of growth can provide bacteria, including probiotics, with means to overcome lethal conditions, including antimicrobial treatments, host immune defenses, and changes in pH, salt, temperature and nutrients (Flemming et al., 2016). Biofilms comprise cells enclosed in an extracellular matrix (consisting of nucleic acids, exopolysaccharides (EPS), lipids and/or proteins) and typically display adherent growth on either abiotic or natural surfaces (Flemming and Wingender, 2010). Probiotics must be consumed at least daily to obtain most of their benefits, and new probiotic supplements prepared as biofilms, e.g., in biocompatible microspheres or encapsulated in microcapsules, could offer longer lasting probiotic effects compared to those prepared from free-grown cells (Cheow and Hadinoto, 2013; Cheow et al., 2014; Olson et al., 2016).

One of the most documented and utilized probiotic *Lactobacillus* strains, *Lactobacillus rhamnosus* GG, is known to adhere to the human intestinal mucosa via pilus (encoded by *spaCBA*) extending from its cell surface and to persist for more than a week in the gastrointestinal tract (GIT) of healthy adults (Kankainen et al., 2009). EPS is another factor that plays an important role as a protective shield against host innate defense molecules to improve adaptation in the GIT (Lebeer et al., 2011a). However, reduced EPS synthesis has been linked to the increased adherence and biofilm formation of GG, which by uncovering specific adhesins necessary for biofilm formation, enabled the enhanced biofilm growth of this strain (Lebeer et al., 2009). The SpaCBA-pilus adhesin, which mediates the direct interaction with the host and abiotic surfaces, and MabA (the modulator of adhesion and biofilm), which strengthens the biofilm structure, are considered the central factors that mediate the biofilm formation of GG *in vitro* (Lebeer et al., 2007b; Velez et al., 2010). While the presence of biofilms in the colonic microbiome has been reported in several studies, GIT-associated probiotic biofilms have been found in specific niches of certain animal hosts (Lebeer et al., 2011b; de Vos, 2015). GG can grow as a biofilm on inert substrates (Lebeer et al., 2007a,b; Savijoki et al., 2011) and integrate well in a multispecies biofilm model with the potential to inhibit the growth of some cariogenic species (Jiang et al., 2016). However, systematic studies aiming to uncover all surface-bound proteins on GG biofilms have not been conducted.

We previously demonstrated that the biofilm formation of GG in MRS medium under microaerophilic and anaerobic (5% CO<sub>2</sub>) conditions was protein-mediated (Savijoki et al., 2011), indicating

that cell surface-associated proteins most likely affected the biofilm formation of this strain. In a multispecies biofilm model, GG was shown to reach high viable cell numbers with glucose or sucrose as the carbon source (Jiang et al., 2018). Glucose and fructose can enhance the survival of GG in simulated gastric juice at pH 2.0 (Corcoran et al., 2005), while fructose also contributes to the *in vitro* adherence and antimicrobial activity of this probiotic (Lee and Puong, 2002; Jiang et al., 2015). These simple carbohydrates were recently found to prevent the colonization of a gut commensal bacterium, *Bacteroides thetaiotaomicron*, in the gut, an effect that was not observed with prebiotic fructo-oligosaccharides (Townsend et al., 2019).

The present study aimed to uncover the effects of two simple carbohydrates, glucose and fructose, on the total surface-associated antigenicity of GG growing in planktonic and biofilm states. To explore these findings further, the surfaceome compositions from the same cells were compared, and some industrially relevant features were verified with phenotypic analyses. To the best of our knowledge, this is the first systematic study exploring surfaceomes of probiotic biofilms and demonstrating the importance of growth mode and carbon source in coordinating the adherent and industrial features of GG.

## MATERIALS AND METHODS

### Culture Media

*Lactobacillus rhamnosus* GG was routinely grown on commercial MRS agar (BD, Franklin Lakes, United States) prior to propagation in modified MRS broth for planktonic or biofilm cultivations. The composition of this modified MRS was as follows: 10 g/L tryptone pancreatic digest of casein, 10 g/L beef extract powder, 5 g/L Bacto™ yeast extract, 1 g/L Tween 80, 2 g/L ammonium citrate tribasic, 5 g/L sodium acetate, 0.1 g/L magnesium sulfate heptahydrate, 0.05 g/L manganese II sulfate monohydrate and 2 g/L dipotassium hydrogen phosphate trihydrate (pH 6.5–7). When appropriate, MRS was supplemented with 2% glucose (glc) (MRS-G) or 2% fructose (frc) (MRS-F) (Sigma-Aldrich, St. Louis, MO, United States) or less (1.75, 1.5, 1.25, 1.0, 0.75, 0.5, 0.25, 0.1, or 0.05%).

### Biofilm Formation and Quantification

GG colonies from MRS agar plates were suspended in MRS supplemented with glc or frc at desired concentrations to obtain an OD<sub>600</sub> = 0.15–0.2, from which 200 μL was removed and added to flat-bottomed 96-well plates (FALCON; Tissue Culture Treated, polystyrene, Becton Dickinson), and the plates were incubated at 37°C under anaerobic conditions (5% CO<sub>2</sub>) for 24 h, 48 h or 72 h. Biofilm formation efficiency was assessed with crystal violet staining essentially as previously described (Sandberg et al., 2008). Briefly, the non-adherent cells were removed from the wells, and the biofilm cells were washed twice with deionized H<sub>2</sub>O. Adherent cells were stained with 200 μL of the crystal violet solution (0.1%, w/v) (Sigma-Aldrich, Munich, Germany) for 30 min at RT. Excess stain was removed by washing the cells twice with deionized H<sub>2</sub>O, and the stained cells were

suspended in 200  $\mu$ L of 30% acetic acid by shaking at RT (400 r.p.m. for 30 min). The density of the biofilms was recorded at 540 nm using an ELISA reader (LabSystems Multiskan EX, Thermo Scientific, Wilmington, DE, United States). Biofilm experiments were performed several times, using at least eight technical replicates.

## LIVE/DEAD Staining of Biofilms and Confocal Microscopy

GG cells were suspended in MRS-G (2% glc) or MRS-F (2% frc) to obtain  $OD_{600} \sim 0.15\text{--}0.2$ , from which 4 mL was added to uncoated 35 mm glass bottom dishes (MatTek, Ashland, MA, United States). Dishes were incubated at 37°C under anaerobic conditions (5%  $CO_2$ ) for 48 h for biofilm formation. Non-adherent cells were removed, and adherent cells were subjected to LIVE/DEAD viability staining using 5  $\mu$ M of Syto9 and 30  $\mu$ M of propidium iodide (PI) according to the manufacturer's instructions (LIVE/DEAD<sup>®</sup> BacLight<sup>™</sup>, Molecular Probes, Life Technologies, Thermo Scientific, Wilmington, DE, United States). Fluorescence images were captured with Zeiss LSM510 META confocal microscope using Zeiss LSM 3.2 software (Zeiss GmbH, Oberkochen, Germany). All biofilms were analyzed in duplicates.

## 1-DE Immunoblotting

Samples from planktonic and biofilm cells for 1-DE (SDS polyacrylamide gel electrophoresis) and immunoblotting were prepared as follows. GG cells were suspended in MRS-G or MRS-F to obtain an  $OD_{600} = 0.15\text{--}0.2$ . The cell suspensions were split in two; half (2.5 mL) of the suspension was cultured under planktonic conditions (Falcon tubes) and half (2.5 mL/ tube) was cultured under biofilm-formation conditions (2.5 mL per well in a flat-bottomed 24-well plate; FALCON – Tissue Culture Treated, Polystyrene, Becton Dickinson) at 37°C in the presence of 5%  $CO_2$ . The cell densities of planktonic cultures and biofilms, after suspending the adherent cells in fresh MRS, were measured at 600 nm. Surfaceome proteins from planktonic cells (1.5 mL) after overnight incubation were harvested by centrifugation (4000  $\times$  g, 3 min, 4°C). Cells were washed once with ice cold 100 mM sodium acetate buffer (pH 4.7). Cells from biofilm cultures after 48 h of incubation were harvested by removing non-adherent cells and washing adherent cells with ice cold acetate buffer as above. Cells normalized to equal cell densities were centrifuged (4000  $\times$  g, 3 min, 4°C) and then suspended gently in Laemmli buffer (pH 7.0) as described earlier (Jakava-Viljanen et al., 2002). Cells were incubated in Laemmli buffer on ice for 15 min and then an additional 5 min at RT. Supernatants were recovered by centrifugation (4000  $\times$  g, 3 min, 4°C) and equal volumes from each sample were subjected to 12% TGX<sup>™</sup> Gel (Bio-Rad, Hercules, CA, United States) electrophoresis (1-DE) using 1 $\times$  Tris-glycine-SDS as the running buffer. After 1-DE, proteins were transferred onto a PVDF membrane using the TransBlot Turbo<sup>™</sup> Transfer System (Bio-Rad, Hercules, CA, United States) according to the manufacturer's instructions. The membrane was then probed first with antibodies (1:4000) detecting surface-associated factors of GG (Espino et al., 2015)

and then with IRDye<sup>®</sup> 800CW goat anti-Rabbit IgG (LI-Cor<sup>®</sup> Biosciences, Lincoln, NE, United States) (1:20000). After probing, the membrane was blocked using Odyssey Blocking buffer and washed with PBS (phosphate buffered saline, pH 7.4) according to the instructions provided by LI-Cor<sup>®</sup> Biosciences. The cross-reacting antigens were detected and quantified using an Odyssey<sup>®</sup> infrared imaging system (LI-Cor<sup>®</sup> Biosciences, Lincoln, NE, United States) and the AlphaView Alpha View 3.1.1.0 software (ProteinSimple, San Jose, CA, United States), respectively. The experiment was repeated three times (each with two technical replicates).

## Mucus Adhesion Assay

Adhesion to mucus was carried out as described previously (Vesterlund et al., 2006; Kainulainen et al., 2013). GG was grown in MRS-G and MRS-F with H<sup>3</sup>-thymidine for metabolic labeling in planktonic and biofilm forms as described above in section 2.4 (1-DE immunoblotting). Briefly, the planktonic and biofilm cells were first washed with a low pH buffer (100 mM sodium acetate, pH 4.7), which prevented the release of adhesive moonlighting proteins (cytoplasmic proteins) from the cell surfaces. Then, the washed cells were allowed to bind the porcine mucin immobilized onto microtiter plate wells. After washing the cells to remove non-adherent cells, the radioactivity of the adherent cells was measured by liquid scintillation, and the percent of bacterial adhesion was determined by calculating the ratio between the radioactivity of the adherent bacteria and that of the added bacteria. The experiment was repeated twice with four to five technical replicates. An unequal variance *t*-test was used to determine significant differences between selected samples.

## Indirect ELISA for Detecting Changes in SpaC Abundance

Planktonic and biofilm GG cells were grown on MRS-G and MRS-F and washed with sodium acetate buffer as above. Washed cells at the same density were treated with 10  $\mu$ M 4,6'-diamidino-2-phenylindole (DAPI; Molecular Probes, Thermo Scientific, Wilmington, DE, United States) to stain all bacterial populations and with antiserum raised against His<sub>6</sub>-SpaC to detect SpaC expression. Antiserum against purified His<sub>6</sub>-SpaC of *L. rhamnosus* GG was raised in rabbits using routine immunization procedures as described previously (Tytgat et al., 2016). The staining was carried out by using indirect immunofluorescence as described previously (Kainulainen et al., 2012) with minor modifications. Briefly, GG cells were collected by centrifugation, washed once with 100 mM Na-acetate buffer (pH 4.7) and fixed with 4% (wt/vol) paraformaldehyde in phosphate buffered saline (PBS; pH 4.0) prior to detection with anti-His<sub>6</sub>-SpaC primary antibody and Alexa-488 (Invitrogen)-conjugated goat anti-rabbit IgG (1  $\mu$ g/ml) secondary antibody and DAPI counterstain. After staining, the optical density ( $OD_{600}$ ) of the cells was adjusted to 1.0 with washing buffer, and the intensity of the fluorescence in the samples was measured using the Victor3 1420 multilabel counter (PerkinElmer, Waltham, MA, United States). The experiment was repeated twice, each with five technical replicates.

An unequal variance *t*-test was used to determine significant differences between selected samples.

## Cell-Surface Shaving and LC-MS/MS Analyses

Surfaceome analyses were conducted with GG cells cultured in planktonic (24 h; stationary phase) and biofilm states (48 h) in MRS-G and MRS-F at 37°C under microaerophilic (5% CO<sub>2</sub>) conditions. Biofilms were formed using flat-bottomed 24-well plates with 2.5 mL of the indicated media containing suspended GG cells (OD<sub>600</sub> = 0.1) per well as described above. After 48 h of incubation, non-adherent cells were discarded, and the adherent cells were washed gently with ice-cold 100 mM Tris-HCl (pH 6.8). Pelleted cells suspended gently in 100 μL of TEAB were mixed with 50 ng/μL of sequencing grade modified porcine trypsin (Promega, Madison, WI, United States), and digestions were incubated at 37°C for 15 min. Released peptides and trypsin were recovered by filtration through a 0.2 μm pore size acetate membrane by centrifugation (7000 × *g*, 2 min, +4°C), and the digestions were further incubated for 16 h at 37°C. The cell samples from planktonic cultures were harvested by centrifugation (7000 × *g*, 2 min, +4°C) and subsequently washed and treated with trypsin as described above for biofilm cells. Digestions were stopped by adding trifluoroacetate (TFA) to a final concentration of 0.6%. The peptide concentrations were measured using a Nano-Drop (ND 1000, Thermo Scientific, Wilmington, DE, United States) at 280 nm. For each growth mode, three biological replicate cultures were used.

Trypsin-digested peptides were purified using ZipTips (C18) (Merck Millipore, Burlington, MA, United States), and equal amounts of the peptide samples were subjected to LC-MS/MS using an Ultimate 3000 nano-LC (Dionex) and QSTAR Elite hybrid quadrupole TOF mass spectrometer (Applied Biosystems/MDS Sciex) with nano-ESI ionization as previously described (Espino et al., 2015). The MS/MS data were searched against the concatenated GG protein database composed of the target (Acc. No. FM179322; 2944 entries) (Kankainen et al., 2009) and the decoy protein sequences using the Mascot (Matrix Science, version 2.4.0) search engine through the ProteinPilot software (version 4.0.8085). The Mascot search criteria were based on trypsin digestion with one allowed mis-cleavage, fixed modification of carbamidomethyl modification of cysteine, variable modification of oxidation of methionine, 50 ppm peptide mass tolerance, 0.2 Da MS/MS fragment tolerance and 1+, 2+, and 3+ peptide charges. The false discovery rate (FDR) percentages calculated using the formula  $2 \times n_{reverse} / (n_{reverse} + n_{forward})$  (Elias and Gygi, 2007) indicated FDRs < 4% in each data set. The raw Mascot proteomic identifications and associated files are freely downloadable from the Dryad Digital Repository (doi: 10.5061/dryad.15534h9).

## Protein Identifications and Surfaceome Comparisons

Mass spectra from each replica sample were searched both separately and combined against the indicated protein database.

Proteins with Mascot score (ms) ≥ 30 and *p* < 0.05 and identified in at least 2/3 replicates were considered high quality identifications and used to indicate condition-specific identifications and relative protein abundance changes. The emPAI (exponentially modified Protein Abundance Index) values of the high confidence identifications were used to estimate protein abundance changes; emPAI is considered roughly proportional to the logarithm of the absolute protein concentration, which allows label-free and relative quantitation of the protein pairs (Ishihama et al., 2005). Principle component analysis (PCA) of the emPAI values was performed with IBM SPSS Statistics v.24. Missing values were substituted with half minimum emPAI value for each protein identified in at least 2/3 replicates in at least one of the conditions using MetImp 1.2<sup>1</sup> (Wei et al., 2018a,b) (**Supplementary Table S1**). Two proteins with zero variance (YP\_003172193.1; YP\_003172584.1) were excluded. PCA of the imputed emPAI data was carried out utilizing Varimax rotation with Kaiser normalization.

## Proteome Bioinformatics

Theoretical molecular weights (MW) and isoelectric points (pI) for the identified proteins were acquired using the Protein Manipulation Suite Server v. 2.0 at <https://www.genscript.com/sms2/proteiniep.html> (Stothard, 2000). The presence of classical secretory motif (signal peptide) and lipobox was predicted using the SignalP Server v. 5.0 at <http://www.cbs.dtu.dk/services/SignalP/abstract.php> (Almagro Armenteros et al., 2019). The cellular location for each protein was predicted using the PSORTb Server v. 3.0 at <https://www.psort.org/psortb/> (Yu et al., 2010) and the number of potential transmembrane domains (TMDs) with the TMHMM Server v. 2.0 at <http://www.cbs.dtu.dk/services/TMHMM/> (Krogh et al., 2001). The identified proteins with plausible moonlighting function/entering the extracellular milieu via non-classical route were predicted using the SecP Server v. 2.0 at <http://www.cbs.dtu.dk/services/SecretomeP/> (Bendtsen et al., 2005). UniProt/Proteomes<sup>2</sup> with the GG proteome ID UP000000955 (UniProtKB, 2,832) with Gene Ontology (GO) IDs was used to link biological process, molecular function and cellular component to each identified protein.

## Analysis of Surface-Associated Aminopeptidase Activities

Cell surface-associated aminopeptidase activity (PepN and PepC) was determined from planktonic and biofilm cells cultured in the presence of 2.0 and 0.5% glc and frc for 24 h (planktonic and biofilm cells) and 48 h (biofilm cells) using a previously reported method (Varmanen et al., 1994) with the following modifications. Briefly, biofilm and planktonic cells (1.8 mL) obtained from 10 mL cultures were washed as described above and then suspended in 1 mL of cold 100 mM Tris-HCl buffer, pH 6.8. The optical density of each sample was measured at 540 nm. The incubation mixture contained 1 mM L-leucine-*para*-nitroanilide (Leu-*p*NA) substrate in

<sup>1</sup><https://metabolomics.cc.hawaii.edu/software/MetImp/>

<sup>2</sup><https://www.uniprot.org/proteomes/>

200  $\mu$ l of the cell suspension. The inhibitory effect of the metal-ion chelator EDTA was examined by incubating the cell suspension with 5 mM EDTA for a few minutes prior to the addition of Leu-pNA. Reactions were incubated at 37°C for 5–25 min and stopped with 800  $\mu$ l of 30% (v/v) acetic acid. After centrifugation (8000  $\times$  g, 5 min), the absorbance was measured at 410 nm. The specific aminopeptidase activity was calculated by dividing the absorbance change at 410 nm by the reaction time used for Leu-pNA hydrolysis and the optical density of the cells (OD<sub>540</sub>). An unequal variance *t*-test was used to determine significant differences between selected samples.

## RESULTS

### Biofilm Formation of GG on Fructose and Glucose

Biofilm formation of GG was first tested at three time points (24, 48, and 72 h after inoculation, hpi) in MRS-G and MRS-F (2% glc and 2% frc) and MRS without carbohydrate, which indicated that frc stimulated biofilm formation by approximately 2-fold compared to glc at each time point tested (**Figure 1A**). The highest biofilm masses in MRS-F and MRS-G were detected at 48 and 72 hpi, respectively (**Figure 1A**). The cell viability analysis of biofilm cells grown on glass-bottom dishes with both carbon sources revealed that biofilms formed on frc at 48 hpi contained proportionally more living cells than those grown on glc (**Figure 1B**). In addition, the biofilm formation efficiency was higher on hydrophilic polystyrene than hydrophilic glass under the conditions used (data not shown).

### Growth Mode- and Carbon Source-Induced Changes in Cell-Surface Antigenicity

The surface antigenicity of GG cells grown in biofilm and planktonic states in MRS-G and MRS-F was studied by subjecting surface-associated proteins extracted in 1 $\times$  Laemmli buffer to 1-DE combined with immunoblotting using antisera raised against intact GG cells. **Figure 1C** reveals that in each sample, the most intense/abundant cross-reacting antigen signals migrated to approximately 65, 55, 40, and 35 kDa. Comparing the total antigen intensity profiles, reflecting antigen abundances (**Figure 1D**), showed that the presence of frc in the growth medium increased the surface antigenicity by  $\sim$ two-fold in planktonic and  $\sim$  2.5-fold in biofilm cells compared to cells grown on glc. In glc-associated cells, switching from planktonic to biofilm growth had no effect on surface-antigenicity, whereas the surface-antigenicity increased by  $\sim$ 20% after switching from planktonic to biofilm growth in the presence of frc. The presence of Frc in the growth medium resulted in the appearance of unique protein bands at 15 and 20 kDa in both the planktonic and biofilm cell samples, while a higher-molecular weight protein ( $\sim$ 200 kDa) was specific to glc- and frc-biofilm samples. Thus, growing cells in planktonic or biofilm forms on frc increases the overall surface-antigenicity of GG along with the specific

production of small-molecular-weight antigens, while a larger protein was specifically produced by biofilm cells growing on both carbon sources.

### Identifying the Surfaceomes of GG Cultured Under Different Conditions

We previously demonstrated that the biofilm formation of GG is mainly protein-mediated (Savijoki et al., 2011). To explore this further, the surfaceomes of cells cultured in biofilm state were analyzed. For obtaining high amounts of biomass needed for proteome analysis without compromising cell viability, the biofilm samples were collected at 48 hpi (**Figures 1A,B**). According to previous studies the physiology of mature biofilms resembles that of stationary phase planktonic cultures (Stoodley et al., 2002; Folsom et al., 2010). Therefore, the planktonic cell samples for comparative analyses were harvested from cultures at stationary phase (24 hpi). LC-MS/MS based protein identifications ( $p < 0.05$ ) are listed in **Supplementary Table S2**. Four surfaceome catalogs [(ms)  $\geq 30$ ,  $p < 0.05$ ] were generated with each data set showing extensive overlap; 70–94% of the identified proteins were shared between at least two of the replica samples (**Supplementary Table S3**). The total number of high-quality identifications was 245 [(ms)  $\geq 30$ ,  $p < 0.05$ ], consisting 94, 117, 179, and 227 proteins from the glc-planktonic, frc-planktonic, glc-biofilm and frc-biofilm cells, respectively (**Supplementary Table S4**). As no decrease in the colony forming units (CFUs) of the shaved cells was observed (data not shown), we concluded that no significant cell lysis had occurred under the trypsin-shaving conditions used. Thus, comparison of the surfaceome catalogs indicated that the number of proteins at the cell surface of GG increased with frc as the carbon source compared to glc. Similarly, growth in the biofilm state increased the number of protein identifications compared to cells grown in planktonic form, regardless of the carbon source used.

### Multivariate Analysis for Screening Specific Surfaceome Patterns

A principal component analysis (PCA) was performed to identify carbon source- and growth mode-dependent patterns in the surfaceome data. **Figure 2A** shows that all biological replicate samples clustered together well, with four clearly separated and identifiable groups. PC1, correlating with the change in growth mode-, and PC2 with the carbohydrate-dependent changes, suggest that the carbon source had a greater effect on GG during biofilm growth than planktonic growth. This was further explored by Venn diagrams that compared the number of specifically identified proteins (unique to growth mode and/or carbon source) and proteins with emPAI values showing  $\geq 2$ -fold change (**Supplementary Table S4**). Venn diagrams in **Figure 2B** compares the growth-mode and carbon source-associated surfaceomes. The number of specifically identified proteins (not identified from planktonic cells) was 90 and 113 in biofilm cells grown on glc and frc, respectively. In total, 5 and 3 identifications were specific for planktonic cells grown on glc and frc, respectively. In addition, the abundance of 60 and 67 proteins increased  $\geq 2$ -fold in biofilm cells, whereas 2

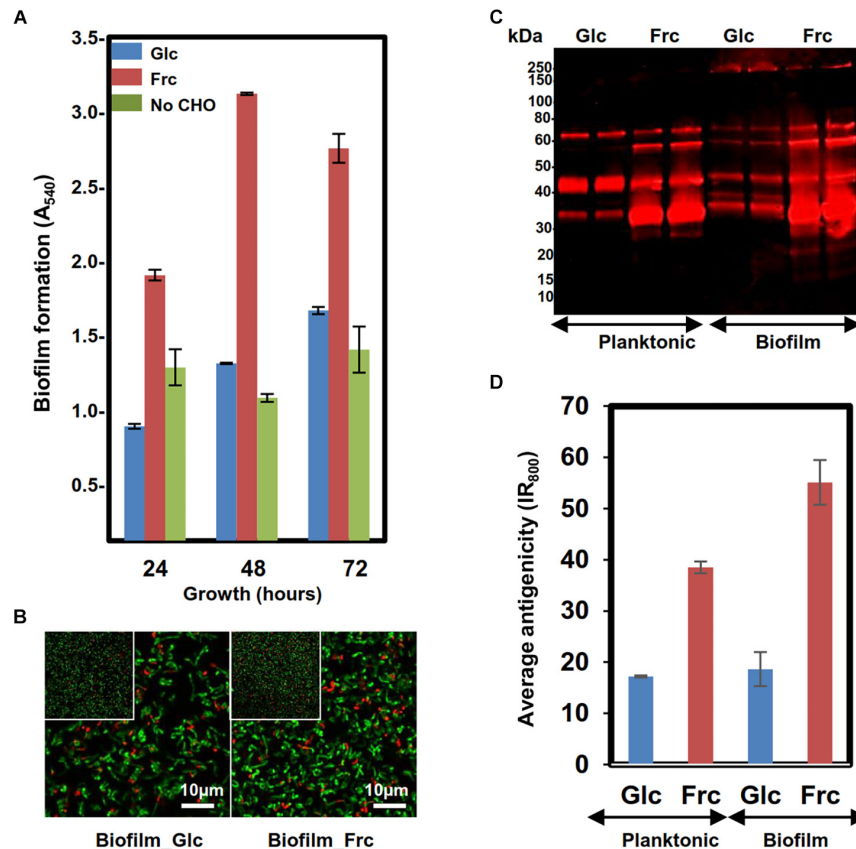


**FIGURE 1** | Assessing the biofilm formation of the GG cells in MRS in the presence 2% glc, 2% frc or without carbohydrate (CHO) under anaerobic conditions (5% CO<sub>2</sub>). **(A)** Biofilm formation efficiency of the GG cells in the presence of frc and glc on flat-bottom polystyrene wells at indicated time points of incubation. **(B)** Fluorescence images of 48 h old biofilms prepared in the presence of glc and frc. Biofilms were stained with the LIVE/DEAD BacLight kit with Syto9 for staining viable cells and PI for dead cells. The scale bar is 10 μm. **(C)** 1-DE immunoblot analysis of planktonic and biofilm GG cells using anti-GG antibodies targeting the surface-associated proteins. The surface proteins were isolated from 24 h old (planktonic) and 48-h-old (biofilms) cells, and the amounts of samples separated by 1-DE were normalized to cell density. Glc and Frc indicate lanes with samples (two technical replicate) grown in presence of glucose and fructose, respectively. The antigen profiles were detected using an Odyssey<sup>®</sup> infrared imaging system. **(D)** Total fluorescence of each 1-DE antigen profile was quantified using the Alphamager gel documentation and image analysis system.

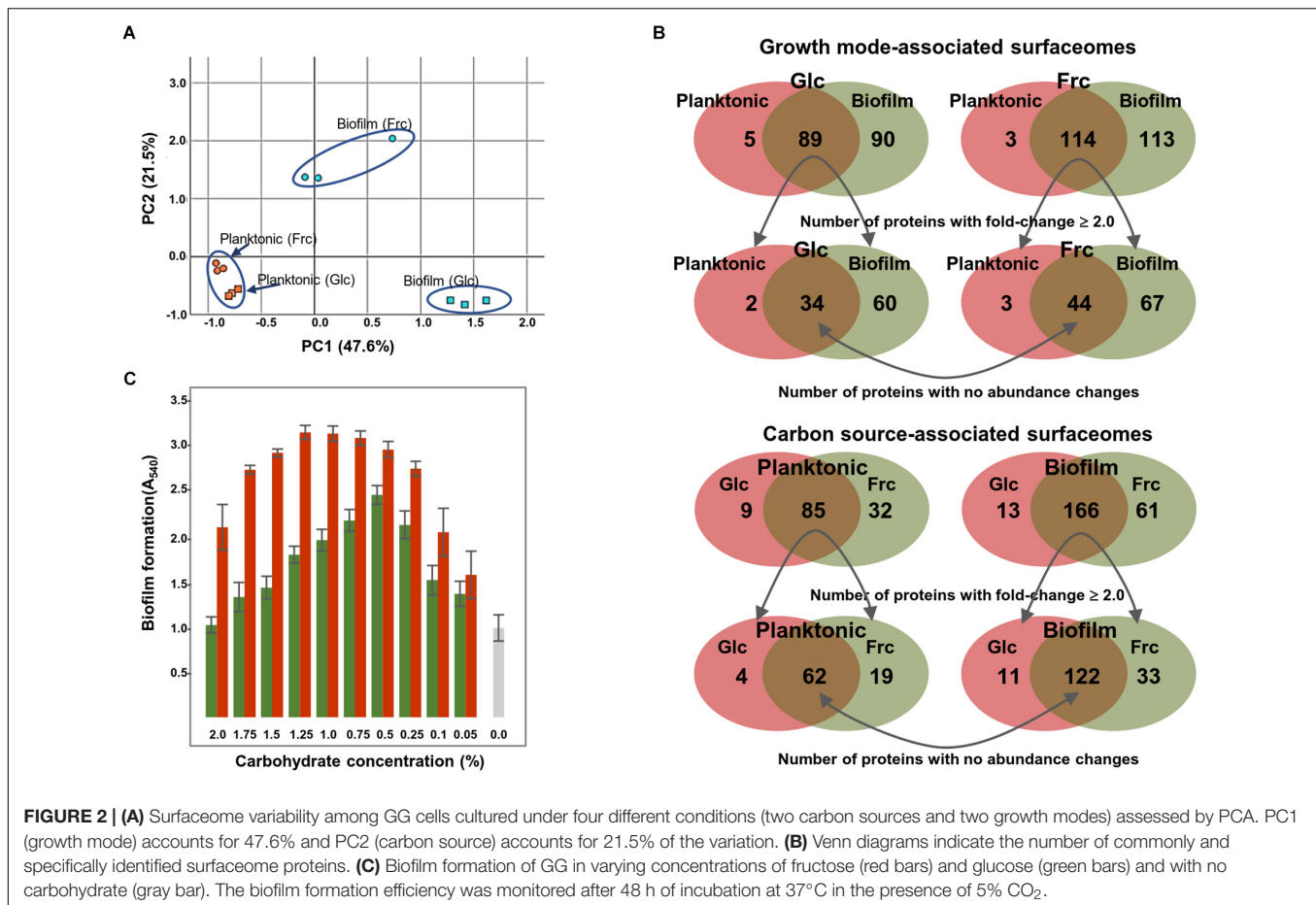
and 3 proteins were more abundant ( $\geq 2$ -fold) in planktonic cells with glc and frc, respectively. With frc as the carbon source, the number of specific identifications (not identified from glc-grown cells) from the planktonic and biofilm cells was 32 and 61, respectively. For glc, 9 and 13 specific identifications were made from the planktonic and biofilm cells, respectively. Four and 19 proteins displayed  $\geq 2$ -times higher abundances in planktonic cells grown of glc and frc, respectively. The number of more abundant proteins with  $\geq 2$ -fold change was 11 and 33 on glc- and frc-associated biofilms. Altogether, the presence of frc in the growth medium resulted in a higher number of specifically identified proteins as well as proteins with increased abundances in comparison to cells grown on glc.

Because Venn diagrams implied that the carbon source affected the number and amount of proteins attached to the biofilm surfaces, we also explored the biofilm formation efficiency in the presence of varying carbohydrate concentrations. **Figure 2C** shows that frc enhanced the biofilm formation over a wider concentration rate compared to glc. However,

0.5% glc produced the thickest biofilms at 48 hpi, while over two-fold higher concentrations of frc were required to achieve the thickest biofilms under the same conditions. Furthermore, optical densities (at 600 nm) of the formed biofilms grown on different carbohydrate concentrations revealed only marginal changes in cell densities, indicating that increased biofilm formation was not accompanied by an increased number of cells (data not shown).

### Categorizing Condition Specific Protein Identifications and Changes in Protein Abundances

Based on the proteome bioinformatics the identified proteins were next divided according to their predicted secretion motifs, subcellular location and cellular functions (**Supplementary Table S4**). Based on this categorization 48 proteins were predicted to be exported via the classical and 68 via the non-classical secretion pathway. For majority of the identifications the proteome bioinformatics tools imply



cytoplasmic or cytoplasmic/membrane location. Next, the most distinctive protein abundance variations, including condition-specific identifications and proteins with abundance change  $\geq 2$ -fold between the indicated conditions were selected for visual illustration by heatmaps; **Figure 3** shows relative abundance changes estimated for classical surface proteins and known/adhesive moonlighters and **Figure 4** candidate moonlighting proteins. Altogether, these proteins could be categorized into three groups: (i) the classically secreted surface adhesins, transporters and enzymes, (ii) known surface-associated moonlighters with adherence features, and (iii) predicted and new candidate moonlighters lacking established extracellular function. The known and candidate moonlighters were the dominant protein group among the detected surfaceomes. Among the identified putative moonlighters, the ribosomal proteins r-proteins (42 proteins), PTS/ABC-type transporter proteins (17 proteins; several OppA paralogs) and amino acid tRNA synthetases (10 proteins) formed the largest protein groups.

#### Protein identifications specific to one of the four tested conditions

The greatest proportion (35 proteins) of the one-condition specific identifications was obtained from the frc-biofilm cells. The proteins identified only from frc-biofilm cells

but not from any other sample type included known and candidate moonlighters (e.g., RbFA, PDHA, GreA, GPD, FrIB, IF-2, and AlaS), Clp family chaperones (ClpL, ClpA, and ClpC) and a PepN aminopeptidase, which were all proposed to be present at relatively high abundances. Seven small molecular weight (6–33 kDa) putative moonlighters (YP\_003170092.1, YP\_003170859.1, YP\_003170536.1, YP\_003171217.1, YP\_003171101.1, YP\_003172119.1, and YP\_003170467.1) were also found to be specific to frc-biofilm surfaces. The classical surface proteins, such as a 70-kDa penicillin-binding protein (PbB3) and a 28-kDa Aes lipase, were specific to frc-biofilm surfaces and, based on the emPAI values were predicted to be produced at low levels under these conditions. Leucyl-tRNA synthetase (LeuS) and glutamine transport (GlnQ) were specifically identified from glc-biofilm surfaces. Protein identifications specific to planktonic cells growing on frc included the SpaC pilin subunit, encoded by the *spaCBA* pilin operon (Kankainen et al., 2009).

#### Protein identifications specific to growth mode

In total, 3 and 47 proteins were detected as specific to planktonic and biofilm cell growth, respectively, independent of the carbon source. Planktonic-specific identifications included the classically secreted 73-kDa lectin-binding protein and ClpB, a candidate moonlighting Clp family ATPase. Classical surface-proteins

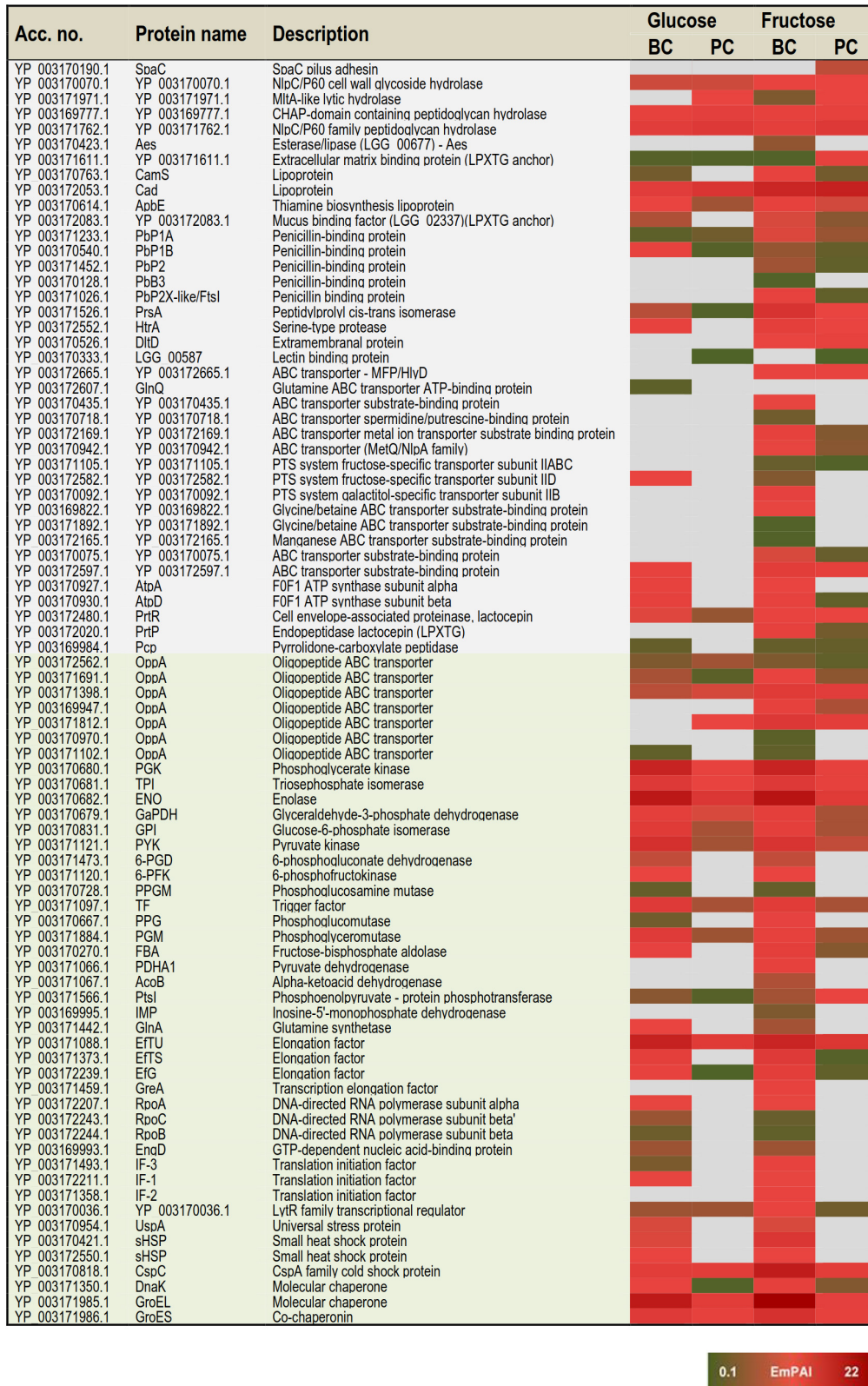


**FIGURE 3** | A heat map comparing the most distinctive protein abundance changes (estimated by the emPAI values) among the classical surface proteins anchored to cell-wall/-membrane via motifs or domains (names shaded in gray) and among known and/or adhesive moonlighters (names shaded in light green). Red and green refer to higher and lower protein abundances, respectively.





0.1 EmPAI 22

**FIGURE 4** | A heat map comparing the most distinctive protein abundance changes (estimated by the emPAI values) among the predicted moonlighters. Red and green refer to higher and lower protein abundances, respectively.

specific to biofilm cells included one of the OppA transporter paralogs (YP\_003171102.1) and AtpA, a subunit of the F-ATPase (F<sub>1</sub>F<sub>0</sub> ATPase). Several known and putative moonlighters were also specifically identified from biofilm cell surfaces. These included seven amino acid tRNA synthetases (Thr, Met, Asn, Ser, Glu, Lys, and Asp); 11 known (D-LDH, PPGM, 6-PGD, UspA, IF-1, 6-PFK, RpoB/C, GlnA, PepA, and EngD); and 13 predicted moonlighters (RpsF, RplP, RpsQ, RpmE2, RplT, RpmG, RplM, RpsC, RplF, RplR, RmlA, RmlC, and RmlD). Among the predicted moonlighters, RmlA, RmlC, and RmlD are encoded by the four-gene (*rmlABCD*) operon involved in dTDP-rhamnose biosynthesis.

#### Protein identifications specific to available carbon source

From the two carbon sources, *frc* was found to induce specific surfaceome changes similar in both the planktonic and biofilm cell surfaces, whereas only one *glc*-specific identification (prolyl-tRNA synthetase-ProS) was shared by the planktonic and biofilm cells. The *frc*-specific identifications included classical surface proteins, such as the lactocepin (PrtP), an extramembranal protein (DltD), a tellurite resistance protein (TelA), five ABC/PTS-type transporters mediating type I protein secretion (MFP/HlyD), amino acid (OppA)/metal ion intake/output proteins (YP\_003172665.1, YP\_003169947.1, YP\_003169947.1, YP\_003170942.1, YP\_003172169.1, YP\_003170075.1, and YP\_003171105) and two penicillin-binding proteins (PbP2 and PbP2X-like/FtsI). In addition, two phosphoglycerol transferase (MdoB) paralogs of different sizes (78 and 84 kDa) and an r-protein, RplX, were detected as candidate moonlighting proteins specific to *frc*-associated cells. From these, the greatest differences were associated with RplX, the ABC transporters for metal ion binding (YP\_003172169.1) and oligopeptide uptake (OppA, YP\_003169947.1), the 78-kDa MdoB paralog and the penicillin-binding proteins PbP2X-like and PbP2, which all displayed over two-fold higher abundances during biofilm growth compared to planktonic growth on *frc*.

#### Growth mode-induced protein abundance changes

Planktonic- or biofilm growth-induced surfaceome changes independent of the carbon source used were considered growth mode-induced changes. Twenty-nine proteins showed similar abundance levels in the *glc*- and *frc*-biofilm cells, and were higher ( $\geq 2$ -fold) in abundance compared to the *glc*- and *frc*-planktonic cells. The greatest differences in abundance were detected for candidate moonlighters, such as an elongation factor – EfG ( $> 8.0$ -fold increase), an 8-kDa hypothetical protein – YP\_003172198.1 (with  $\sim 6.0$ -fold increase), an aminopeptidase – PepC (with  $\sim 5.0$ -fold increase) and a ClpP caseinolytic peptidase ( $> 2.0$ -fold increase). Known moonlighters (PGK, TPI, L-LDH, GaPDH, and RpoA) and 21 r-proteins (RplR, RplO, RpsG, RplJ, RplU, RplQ, RpsD, RpsE, RpsR, RpsD, RpsE, RpsB, RpsS, RpsA, RpsM, RpsH, RplK, RpsL, RplN, RplK, and RplB) were less abundant but still over 2-fold more abundant on biofilm than on planktonic cell surfaces. Only one of the OppA paralogs (YP\_003171102.1) was

found to be  $\sim 5$ -times more abundant on planktonic cells on both carbon sources.

#### Effect of carbon source on biofilm-induced protein abundance changes

In total, 61 proteins more abundant in *glc* and *frc* biofilms than in planktonic cells were divided into four groups as follows: (i) Biofilm-induced proteins showing greater relative abundance difference between planktonic and biofilm growth modes when grown on *glc*. This group included twenty-two proteins and 14 proteins with  $> 5$ -fold higher differences in abundance and included the classically secreted penicillin-binding protein (PbP1B) as well as several known and predicted moonlighters (DnaK, L-LDH, PYK, PGM, GBI, RplA, RplD, RpsE, RpsB, RplQ, RpsG, and the 8-kDa YP\_003172198.1). (ii) Biofilm growth induced proteins more abundant on *glc*-biofilm than on *frc*-biofilm cell surfaces included dihydrolipoamide acetyltransferase ( $\sim 4.7$ -fold increase), a potential Com\_YlBF family protein predicted to ensure proper biofilm formation ( $\sim 2.7$ -fold increase) and five r-proteins (RplK, RplB, RplN, RpsF, and RpmF) with fold-changes ranging from 2.4 to 4.6. (iii) Biofilm-induced proteins showing greater relative abundance difference between planktonic and biofilm growth modes when grown on *frc*. The majority of these were identified as known and candidate moonlighters (EfTS, GroEL, AtpD, FBA, RplV, RpsR, and CspC), with fold-change 4–15 and with EfTS ( $\sim 15$ -fold increase) and GroEL ( $\sim 9$ -fold) displaying the greatest changes in abundance. The classical surface-proteins, including the PrtP protease (specific to *frc*-cells) and the lipoprotein CamS ( $\sim 4$ -fold increase), were predicted to be more abundant on *frc* cells than on *glc* cells. (iv) Biofilm growth induced proteins more abundantly produced on *frc*- than on *glc*-associated biofilm cell surfaces included five classical surface proteins, which included one of the OppA paralogs (YP\_003171812.1), the PrsA chaperone/foldase, the serine-proteases PrtP and HtrA and the CamS lipoprotein. Of these, OppA ( $> 15$ -fold increase), PrsA ( $\sim 7$ -fold increase) and PrtP ( $\sim 4$ -fold increase) displayed the greatest changes in abundance. In total, nine possible moonlighters were also more abundantly produced ( $\geq 4$ -fold) on *frc*-biofilm cell surfaces, including an 18 kDa small heat shock protein (sHSP), a cold-shock protein (CspC), two amino acid tRNA synthetases (LysS and AspS), RpsR, phosphoglucomutase (PPG), and a dTDP-glucose-4,6-dehydratase (RmlB, encoded by the *rmlABCD* operon). In addition, a dTDP-4-dehydrorhamnose reductase – RmlD, with a  $> 2.0$ -fold change in abundance, was also identified from the *frc*-biofilm cells.

#### Carbon source-induced changes in planktonic cultures

Carbon source-dependent changes in planktonic cell surfaces could be divided into two groups. (i) Proteins predicted to be more abundant on cells growing on *frc* included the extracellular matrix-binding protein (YP\_003171611.1) with  $> 8$ -fold higher abundance. Another classical surface protein, PrsA, and two moonlighters (PtsI and RplC) were also predicted to be  $\sim 5$ -fold more abundantly produced on *frc* cells. (ii) Proteins predicted to be more abundantly produced in the presence of *glc* included one of the OppA paralogs (YP\_003171812.1), an

MltA lytic hydrolase, a prolyl-tRNA synthetase – ProS, and the AtpD protein.

## Adherence of Biofilm and Planktonic Cells to Porcine Mucus

Because the identification data implied that the growth mode and carbon source in the growth medium could affect the adherence features of GG, we investigated the mucus-binding ability of the planktonic and biofilm cells grown on glc and frc. **Figure 5A** indicates that the biofilm cells grown on frc displayed the highest level of adherence, while planktonic cells grown on glc were the least adherent. The frc biofilms demonstrated a mucus-binding ability that was ~2-fold more efficient than that of the glc-associated planktonic cells;  $p = 0.037$ ). The possible role of the SpaC-adhesin, the tip pilin of the SpaCBA pilus known to mediate key interactions with the human mucus (Kankainen et al., 2009), in mediating the frc-stimulated adherence was assessed next by testing the adherence of the GG cells in the presence of anti-SpaC antiserum. **Figure 5A** indicates that the presence of SpaC antibodies markedly decreased the adherence of each type of cell to mucus. Although the final level of adherence detected for these cells was somewhat similar, the biofilm cells grown on frc displayed the greatest SpaC-mediated inhibition, whereas the level of adherence decreased the least in glc-associated planktonic cells. To readdress the possible role of the pilus structure in the observed differences, we also monitored the SpaC abundances on each GG cell type. As shown in **Figure 5B**, the highest abundance of SpaC was detected on the glc-associated biofilm cells, which was > 2-fold ( $p = 4.46e-09$ ) higher than that on the planktonic cells grown on glc and ~2-fold ( $p = 1.15e-07$ ) higher than that on the frc-biofilm cells. Planktonic cells grown on frc displayed the lowest SpaC abundance.

## Whole-Cell Aminopeptidase Activity

Varying abundances detected for predicted cell-surface moonlighters, such as PepN, PepC, PepA, ClpP, and several OppA paralogs, implied differences in the ability of the GG cells to utilize casein/casein-derived peptides for growth. PepN was specific to frc-biofilm cells. PepC was predicted to be equally abundant on the biofilm cells grown on frc and glc and displayed over a 4-fold higher abundance on biofilm than planktonic cells. Comparison of PepN and PepC implies that PepC is produced ~2-fold more on the frc-biofilm cells than PepN on the same cells. To verify these results, we monitored the surface-associated aminopeptidase activity by exposing washed and intact GG cells to a chromogenic substrate, Leu-pNA, a specific substrate for both aminopeptidases (Varmanen et al., 1994). **Figure 5C** confirms the identification findings by showing that the surface-associated aminopeptidase activity of frc-biofilm cells was ~4-fold higher ( $p = 0.001$ ) than that of planktonic cells growing on frc. Changes from glc to frc increased the aminopeptidase activity on both the planktonic and biofilm cell surfaces but led to a proportionally greater increase in the biofilm cell surface. Lowering the carbohydrate concentration to 0.5% increased the aminopeptidase activity in planktonic cells

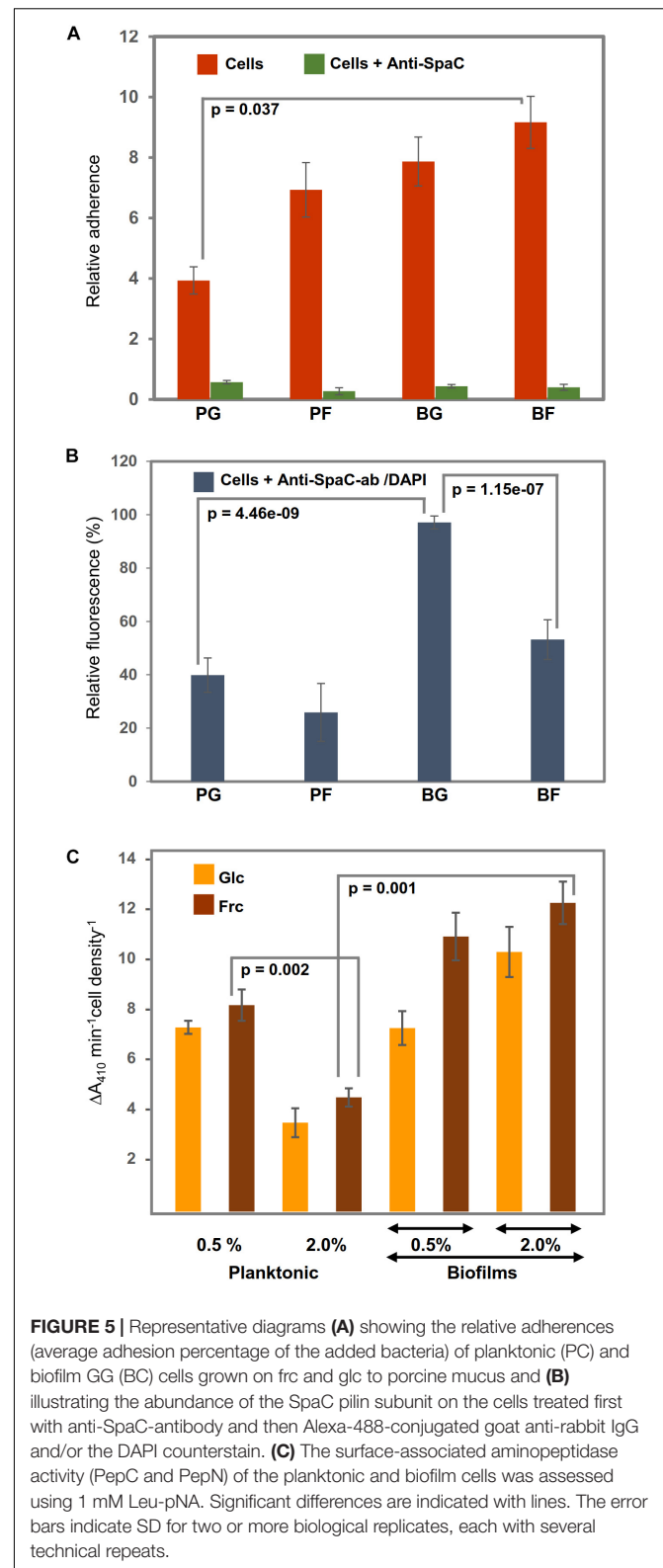


**FIGURE 5** | Representative diagrams (A) showing the relative adhesions (average adhesion percentage of the added bacteria) of planktonic (PC) and biofilm GG (BC) cells grown on frc and glc to porcine mucus and (B) illustrating the abundance of the SpaC pilin subunit on the cells treated first with anti-SpaC-antibody and then Alexa-488-conjugated goat anti-rabbit IgG and/or the DAPI counterstain. (C) The surface-associated aminopeptidase activity (PepC and PepN) of the planktonic and biofilm cells was assessed using 1 mM Leu-pNA. Significant differences are indicated with lines. The error bars indicate SD for two or more biological replicates, each with several technical repeats.

by ~4-fold, while only a slight decrease in the enzyme activity was observed in biofilm cells on both carbon sources. Enzyme activities were also examined in the presence of 5 mM EDTA,

a metal-chelator that inhibits the activity of metallopeptidases such as PepN while not affecting other types of peptidases such as PepC (Varmanen et al., 1994). Since EDTA inhibited only marginally the total aminopeptidase activity only in frc-biofilm cells, PepC is the likely candidate for the hydrolysis of the substrate.

## DISCUSSION

### Carbon Source Controls the Protein-Dependent Biofilm Growth of GG

Environmental signals, such as O<sub>2</sub>, CO<sub>2</sub>, bile, mucins, non-digestible polysaccharides and carbohydrates present in the human GIT, have been shown to affect the GG biofilm formation *in vitro* (Lebeer et al., 2007b; Savijoki et al., 2011). In MRS growth medium, GG produces biofilm, which is completely disintegrated by treatment with proteolytic enzyme (Savijoki et al., 2011), indicating the presence of a large amount of proteins in the biofilm matrix and/or that biofilm formation is protein-mediated. Since both carbon metabolism (Lebeer et al., 2007b) and cell-surface exposed proteins (Savijoki et al., 2011) appear to play a role in biofilm formation, we explored this link further by investigating the effects of glc and frc as carbon sources on the surfaceome composition of GG. Our findings indicated that changing the carbon source from glc to frc resulted in enhanced biofilm formation efficiency of GG *in vitro*. GG is known to exert high *in vitro* adhesion to Intestinal Epithelial Cells (IECs) and biofilm formation capacity on polystyrene and glass (Doron et al., 2005; Lebeer et al., 2007b). Here, our findings demonstrated more efficient biofilm growth on polystyrene than on glass and more efficient biofilm growth with frc than with glc on both inert materials. Crystal violet provides a good detection of biofilm mass, but this dye stains both the bacterial cells and extracellular matrix, including proteins (Santhanalakshmi and Balaji, 2001; Welch et al., 2012). As the tested carbohydrates had only a marginal effect on the cell density, we suggest that the increase in crystal violet staining, instead of showing increased biofilm formation, related directly to changes in the protein abundance of biofilm cells. A similar observation was also made when growing the biofilm cells with varying carbohydrate concentrations; decreased carbohydrate concentrations resulted in thicker biofilms, which did not result from higher cell density (data not shown). Thus, changes in carbon sources and their concentrations regulate the changes in protein abundance on the biofilm cell surfaces.

### Biofilm Growth and frc in Growth Medium Enhance the Protein Export in GG

Examining the cause-effect relationships between the identified surfaceomes revealed that the carbon source played a more important role in the biofilm mode of growth. Conditions of glc limitation have been shown to enhance the biofilm formation of GG (Velez et al., 2010). Here, decreasing the concentration

of both carbon sources in growth medium resulted in similar outcomes. The presence of frc enhanced biofilm formation over wider concentrations than glc. Putative moonlighting proteins, including predicted as well as new candidate moonlighters, were the dominant protein group in the biofilm-associated surfaceomes. Comparing the frc- and glc-associated surfaceomes implied that these non-classical surface proteins are more abundantly present in both the biofilm and planktonic cells growing on frc. These results could be explained by increased cell lysis within the biofilm and the fructose containing cultures or alternatively, be a result of non-classical protein export by a yet unknown pathway. Cell lysis in biofilms is a well-reported phenomenon for model bacteria like *S. aureus* (Rice et al., 2007; Houston et al., 2011; Mashruwala et al., 2017), but remains to be studied in *L. rhamnosus* GG. In this study, three proteins potentially involved in hydrolysis of peptidoglycan and autolysis were identified, NlpC/P60, MltA and a CHAP-domain containing peptidoglycan hydrolase. Of these, NlpC/P60 was previously identified from the surface of exponentially growing *L. rhamnosus* GG cells, while the other two proteins were not detected in that study (Espino et al., 2015). Here, the results indicate constant expression of NlpC/P60 and CHAP-domain containing peptidoglycan hydrolase under the conditions used, whereas MltA appears to be more abundant on stationary phase planktonic cells than on biofilm cells. Thus, while the presence of MltA and the CHAP-domain containing peptidoglycan hydrolase could be linked to increased autolysis in stationary phase and biofilm cells compared to exponentially growing cells, these protein identification results do not support increased autolysis activity as an explanation of higher number of cytoplasmic proteins on biofilm cells compared to stationary phase planktonic cells. The presence of moonlighting proteins on the cell surface or in the culture medium has been reported for several microbial species, and for many of these, the moonlighting activity outside of the cells has been demonstrated (Kainulainen and Korhonen, 2014; Chen et al., 2018). It has been proposed that bacteria recycle conserved cytoplasmic proteins in a pH-dependent manner in the matrix to facilitate interspecies interactions without specifically recognizing the dedicated matrix components of the other species (Foulston et al., 2014). In a recent study, the strongly positively charged r-proteins were shown to be embedded in *S. aureus* biofilm matrix under acidic conditions (Graf et al., 2019). This was proposed to depend on the pH, coordinated by the formation/release of acidic fermentation end-products in the biofilm cells facing oxygen limitation (Graf et al., 2019). In the present study, the pHs of the spent culture supernatants were clearly acidic, pH < 5.0 (data not shown). Thus, while r-proteins were identified as the most abundant moonlighters in the biofilm matrices, we suggest that low pH could have promoted the interactions between the r-proteins and the biofilm cells also in the present study.

In general, the mechanisms underlying export/transport of moonlighting proteins remain unknown (Wang and Jeffery, 2016). In view of this, it is tempting to speculate that the specific appearance of HlyD/MFP in frc-associated cell surfaces indicates the role of this protein in directing moonlighting proteins out of the cell. HlyD is part of a translocon that comprises

HlyB, HlyD, and TolC, which is proposed to coordinate the transport of potential novel proteins by quite different mechanisms (Holland et al., 2016). Overexpression of PrsA, a known surface-associated chaperone or foldase acting on secreted proteins (Kontinen and Sarvas, 1993), on biofilm cells and *frc*-associated cells is another plausible factor contributing to protein secretion under these conditions. This chaperone/foldase is known to enhance protein secretion efficiency in bacteria (Chen et al., 2015) and act on various substrates, ranging from 20 to 80 kDa in size (Jakob et al., 2015). The serine-type surface-protease, HtrA, follows the same abundance trend as PrsA and is another classical surface-protein that could enhance protein secretion in *frc*-associated samples. In bacteria, HtrA is involved in degrading abnormal proteins, processing secreted proproteins and the maturation of native proteins (Poquet et al., 2000), but this protease can also affect biofilm formation and control the presence of surface-associated moonlighters, such as enolase (ENO) and glyceraldehyde-3-phosphate dehydrogenase (GaPDH) (Biswas and Biswas, 2005).

Here, ENO, EftU, TDPA, PGK, and GroEL, each with previously reported adhesive functions (Kainulainen and Korhonen, 2014; Chen et al., 2018), were detected as the most abundant moonlighters in the biofilm cells growing on both carbon sources. In addition, stress response proteins (GroES and DnaK), glycolytic proteins (PGM, PYK, PGK, FBA, GPI, L/D-LDH, GMR, and PDCE2), the elongation factors EftS and EftG, the RNA polymerase subunit RpoA, the translation initiation factor IF1, and the trigger factor (TF), were also detected as relatively abundant on biofilms. The *r*-protein moonlighters (a total of 43 proteins) were the largest protein group among the biofilm-associated surfaceomes, independent of the carbon source used. In addition to their proposed role as biofilm integrity/stability enhancing role, coordinated by the production of acidic fermentation end-products (Graf et al., 2019), some of the identified *r*-proteins may also have other moonlighting functions. The most abundant *r*-proteins were RplX, RpsE, RpsG, RplL, and RplO, from which RplL (the 50S ribosomal protein L7/L12) was predicted to be the most abundant. The high abundance of this *r*-protein during biofilm growth could explain the concomitant presence of another moonlighting protein, EftG, on the biofilm cells at high abundances, as the GTPase activity of EftG is reported to require RplL for ribosomal translocation (Koch et al., 2015). For several *r*-proteins (e.g., L5, L11, L23, L13a, S3, S19, and S27), non-canonical functions ranging from gene expression regulation to subverting pro-inflammatory actions, apoptosis and protection against abiotic stress (Liu et al., 2014; Henderson et al., 2016; Chen et al., 2018) have been proposed. The increased abundance of the TF during the biofilm mode of growth could be explained by the concomitant presence of the ribosomal protein L23. This *r*-protein has been reported to have binding sites for both the TF and the signal recognition particle, which is thought to aid in protein export to the cell membrane (Hoffmann et al., 2010). The specific appearance of several moonlighting aminoacyl-tRNA synthetases (ATRSs) in biofilm cells was also interesting, as these enzymes, unrelated to their primary function, also regulated

gene expression, signaling, transduction, cell migration, tumorigenesis, angiogenesis, and/or inflammation (Son et al., 2014; Chen et al., 2018), thereby forming a novel group of moonlighters in probiotic species.

## Fructose and Biofilm Growth Increase the Surface-Associated Aminopeptidase Activity in GG

Several components of the proteolytic system (several OppA paralogs, PepC, PepN, and PepA) involved in the utilization of milk casein (Savijoki et al., 2011) were identified here as candidate moonlighters with higher abundances on biofilm than planktonic cell surfaces. Among these PepN and the OppA paralogs were more abundant on or specific to the *frc*-associated cell surfaces. The enzymatic assay performed on whole cells using a substrate specific to PepC and PepN confirmed the identification results and indicated that more PepC than PepN is associated with biofilm cells. In addition, the classical surface proteases PrtP and PrtR were predicted to be more abundantly produced on the biofilm cell surfaces. The two identified aminopeptidases are expressed in the cytoplasm, where they act on the oligopeptides that are taken up by the Opp-transport system. Thus, efficient surface-aminopeptidase activity could provide the probiotic with means to speed up growth and adaptation in conditions involving oligopeptides as the carbon source. In a recent study by Galli et al. (2019) GG was utilized as an adjunct starter culture in Camembert-type cheese production, which was found to improve the sensory characteristics of the cheese. While the mechanism behind the GG-mediated flavor formation in cheese remains to be elucidated, the efficient and diversified proteolytic system of the strain could be involved (Galli et al., 2019). It is highly likely that the robust GG cells do not undergo autolysis during cheese making, which makes the cell-surface located moonlighting aminopeptidases C and N interesting objects to be studied further in this context.

Several cytoplasmic proteins have been shown to be selectively sorted into membrane vesicles (MVs), which in some bacteria were shown to contribute to approximately 20% of the whole biofilm matrix proteome, demonstrating that MVs are also important constituents of the biofilm matrices (Couto et al., 2015). Protein targeting to MVs provides an important mechanism exploited by both gram-negative and gram-positive bacteria to export proteins in a protected and concentrated manner to aid neighboring cells or modulate the host immune system. Whether MVs play a role in *L. rhamnosus* GG biofilm formation and surface protein export, remain to be studied.

## Surface-Antigenicity and Adherence of GG by Biofilm Growth in the Presence of *frc*

Comparison of the total antigenicity profiles of GG cells grown in planktonic and biofilm forms on *glc* and *frc* indicated that *frc* as the carbon source increases the abundances of many antigens (~23, 28, 40, and 60 kDa in size) during both growth

modes. We previously demonstrated the presence of several adhesive and antigenic moonlighters at the cell surface of planktonic GG cells grown on *glc* (Espino et al., 2015). In that study, protein moonlighters, such as DnaK (67.2 kDa), GroEL (57.4 kDa), PYK (62.8 kDa), TF (49.8 kDa), ENO (47.1 kDa), GaPDH (36.7 kDa), L-LDH (35.5 kDa), Eftu (43.6 kDa), Adk (23.7 kDa), and UspA (16.8 kDa), were identified as highly abundant and antigenic on planktonic GG cells. The present study suggests that PYK, ENO, GaPDH, TF, L-LDH, Eftu, UspA, DnaK, and GroEL could be produced more during biofilm than planktonic growth, which is also in line with an earlier proteomic study showing that a switch from planktonic to biofilm growth in *L. plantarum* increases the abundances of several stress responses and glycolytic moonlighters (De Angelis et al., 2015). From the identified moonlighters, ENO, IMP, FBA, TDPA, GreA, GroES, and GroEL are plausible factors that aid in biofilm formation in the presence of *frc*, as evidenced by surfaceome predictions.

The *rmlABCD* operon products, involved in the synthesis of O-antigen lipopolysaccharide (Reeves, 1993), could have conferred increased surface antigenicity to GG cells during biofilm growth. Here, all of the operon gene products RmlA, RmlB, RmlC, and RmlD corresponding to glucose-1-phosphate thymidyltransferase, dTDP-4-dehydrorhamnose 3,5-epimerase, dTDP-4-dehydrorhamnose reductase and dTDP-glucose-4,6-dehydratase, respectively, were detected only in biofilm cells and with ~2-fold higher abundances in the presence of *frc*. In some pathogens, L-rhamnose is required for virulence, and the enzymes of the Rml pathway are considered potential targets in drug design (Trent et al., 2006). In view of this, detection of the Rml enzymes as moonlighters is interesting and points toward a novel role of these enzymes at the cell surface of non-pathogenic bacteria. The rhamnose moiety has also been shown to bind specific moonlighters (e.g., ENO and 58 other potential moonlighters) at the bacterial cell surface, proposing that rhamnose-mediated anchoring is a general mechanism for anchoring the moonlighting proteins to the cell surface in bacteria (Daubenspeck et al., 2016).

The identified DltD, encoded by part of the *dltABCD* operon involved in the formation of lipoteichoic acid (LTA), could have increased antigenicity in *frc*-associated GG cells. DltD is a single-pass membrane protein involved in the final transfer of D-alanine residues to LTA on the outside of the cell (Reichmann et al., 2013) that contributes to adherence and biofilm formation (Spatafora et al., 1999; Gross et al., 2001). LTA has been shown to be essential for biofilm matrix assembly and bulk accumulation over time (Castillo Pedraza et al., 2017), and the early stages of biofilm formation necessitates efficient expression of *dltD* (Klein et al., 2012). In addition, a lack of DltD has been linked to poor acid survival in planktonic cells and an inability to form biofilms *in vitro* in the presence of sucrose or glucose (Quivey et al., 2015). As DltD could not be detected in the *glc*-associated planktonic or biofilm cells, we hypothesize that such deficiency might also explain the lower biofilm formation efficiency on *glc* compared to *frc*.

Many of the classical surface proteins may have also contributed to the total antigenicity and/or adherence in the GG cells. The most plausible candidates include lipase and lipoproteins (Aes, AbpE, Cad, and CamS), peptidoglycan hydrolases (e.g., the NlpC/P60), MBF, a lectin-binding protein, penicillin-binding proteins and the pilus protein SpaC. The identification data implies that SpaC is specifically produced during planktonic growth on *frc*. From these proteins, the SpaC adhesin and MBF are best known; the first is produced through the *spaCBA* operon coding for the pilus, the key factor promoting biofilm formation *in vitro* as well as colonization and adherence *in vivo* (Lebeer et al., 2007b, 2012), while MBF has been shown to bind intestinal and porcine colonic mucus, laminin, collagen IV, and fibronectin (von Ossowski et al., 2011; Nishiyama et al., 2015). Additional mucus-adherence assays with each GG cell type in the presence of anti-SpaC antibodies complemented with indirect ELISA monitoring of the SpaC abundances indicated the importance of the pilus adhesin in coordinating the adherence in both the planktonic and biofilm cells. Surprisingly, the *glc*-associated biofilm cells with the highest SpaC abundance did not show the highest mucus binding ability, which was detected for *frc* grown biofilm cells. Possible explanations to this discrepancy include presence of specific factors in biofilm cells grown on *frc*, which could enhance or strengthen the pilus mediated mucus binding. The inability to identify SpaC by LC-MS/MS from biofilm-cells implied that the complex structure of the pilus adhesin together with the overwhelming presence of moonlighting proteins on biofilm cell surfaces could be the reason why the pilus protein was identified only from the planktonic cells. The same reason applies for the lack of MabA among the identified surfaceomes. MabA (LGG\_01865), the modulator of adhesion and biofilm formation, is proposed to strengthen the biofilm structure following the pilus-mediated interaction with the surface (Velez et al., 2010).

A recent study highlighted an important role of *glc* and *frc*, carbohydrates prevalent in the Western diet, in regulating the colonization of a beneficial microbe independent of supplying these carbohydrates to the intestinal microbiota (Townsend et al., 2019). In that study, both *frc* and *glc*, but not prebiotics such as fructo-oligosaccharides, were found to silence the two-component system sensor histidine kinase/response regulator Roc that activates transcription of clustered polysaccharide utilization genes in a widely distributed gut commensal bacterium *B. thetaiotaomicron*. Roc was also suggested to promote gut colonization by interacting with moonlighting proteins such as GPI or glucose 6-phosphate dehydrogenase (Sonnenburg et al., 2006). From these two moonlighters, GPI was detected here as a more abundant protein in biofilm cells with a slight increase in cells grown on *glc*. As the present study compared surfaceomes of cells grown only in the presence of simple carbohydrates, we cannot exclude the possibility that corresponding response regulators (e.g., WalkK) could have been modulated by these carbohydrates and that the two tested carbohydrates could coordinate the colonization of GG *in vivo* in an analogous manner.

## CONCLUSION

The present study provides the first in-depth comparison of the planktonic- and biofilm matrix-associated surfaceomes of GG. We show that cells growing in planktonic and biofilm forms in the presence of simple carbohydrates in growth medium could be used to modify the surfaceome composition of this probiotic. We show remarkable differences among the compositions of the classical and non-classical surface proteins (moonlighters) that have immunomodulatory, adherence, protein-folding, proteolytic or hydrolytic activities. Our study also indicated that the carbon source coordinates protein-mediated biofilm formation, as evidenced by a whole-cell enzymatic assay measuring the surface-associated aminopeptidase activity on cells cultured on different carbon sources and with varying carbohydrate concentrations. The total antigenicity and adherence were higher on biofilm and planktonic cells grown on frc, in which specific surface-adhesins and putative moonlighters were the plausible contributory factors. Our findings also demonstrated the key role of the SpaCBA pilus independent of the growth mode or carbon source used, whereas the increased protein moonlighting is suggested to strengthen the biofilm structures and/or aid in cell-cell interactions. The observed phenotypic variations in *L. rhamnosus* GG potentially includes probiotic (adherence and immunomodulatory) and industrially relevant (proteolytic activity) features. Whether the GG phenotypes could be modulated in the host or in the food conditions remains to be shown.

## REFERENCES

- Almagro Armenteros, J. J., Tsirigos, K. D., Sønderby, C. K., Nordahl Petersen, T., Winther, O., Brunak, S., et al. (2019). SignalP 5.0 improves signal peptide predictions using deep neural networks. *Nat. Biotechnol.* 37, 420–423. doi: 10.1038/s41587-019-0036-z
- Aoudia, N., Rieu, A., Briand, R., Deschamps, J., Chluba, J., Jegou, G., et al. (2016). Biofilms of *Lactobacillus plantarum* and *Lactobacillus fermentum*: effect on stress responses, antagonistic effects on pathogen growth and immunomodulatory properties. *Food Microbiol.* 53, 51–59. doi: 10.1016/j.fm.2015.04.009
- Bendtsen, J. D., Kiemer, L., Fausbøll, A., and Brunak, S. (2005). Non-classical protein secretion in bacteria. *BMC Microbiol.* 5:58. doi: 10.1186/1471-2180-5-58
- Biswas, S., and Biswas, I. (2005). Role of HtrA in surface protein expression and biofilm formation by *Streptococcus mutans*. *Infect. Immun.* 73, 6923–6934. doi: 10.1128/IAI.73.10.6923-6934.2005
- Castillo Pedraza, M. C., Novais, T. F., Faustoferrri, R. C., Quivey, R. G., Terekhov, A., Hamaker, B. R., et al. (2017). Extracellular DNA and lipoteichoic acids interact with exopolysaccharides in the extracellular matrix of *Streptococcus mutans* biofilms. *Biofouling* 33, 722–740. doi: 10.1080/08927014.2017.1361412
- Chen, C., Zabad, S., Liu, H., Wang, W., and Jeffery, C. (2018). MoonProt 2.0: an expansion and update of the moonlighting proteins database. *Nucleic Acids Res.* 46, D640–D644. doi: 10.1093/nar/gkx104
- Chen, J., Gai, Y., Fu, G., Zhou, W., Zhang, D., and Wen, J. (2015). Enhanced extracellular production of  $\alpha$ -amylase in *Bacillus subtilis* by optimization of regulatory elements and over-expression of PrsA lipoprotein. *Biotechnol. Lett.* 37, 899–906. doi: 10.1007/s10529-014-1755-3
- Cheow, W. S., and Hadinoto, K. (2013). Biofilm-like *Lactobacillus rhamnosus* probiotics encapsulated in alginate and carrageenan microcapsules exhibiting enhanced thermotolerance and freeze-drying resistance. *Biomacromolecules* 14, 3214–3222. doi: 10.1021/bm400853d

## DATA AVAILABILITY

The datasets generated for this study can be found in the Dryad Digital Repository, <https://doi.org/10.5061/dryad.15534h9>.

## AUTHOR CONTRIBUTIONS

KS, PV, TN, PS, VK, RS, AF, and JS conceived, designed, and performed the experiments. IM analyzed the data. KS and PV wrote the manuscript. All authors participated in the revision of the manuscript and approved the final version of the manuscript.

## FUNDING

This study was supported by the Academy of Finland (Grant No. 272363 to PV and 285632 to VK) and by Sigrid Juselius Foundation's Senior Reseachers' grant to RS. Open access publication fees were covered by Helsinki University Library.

## SUPPLEMENTARY MATERIAL

The Supplementary Material for this article can be found online at: <https://www.frontiersin.org/articles/10.3389/fmicb.2019.01272/full#supplementary-material>

- Cheow, W. S., Kiew, T. Y., and Hadinoto, K. (2014). Controlled release of *Lactobacillus rhamnosus* biofilm probiotics from alginate-locust bean gum microcapsules. *Carbohydr. Polym.* 103, 587–595. doi: 10.1016/j.carbpol.2014.01.036
- Corcoran, B. M., Stanton, C., Fitzgerald, G. F., and Ross, R. P. (2005). Survival of probiotic lactobacilli in acidic environments is enhanced in the presence of metabolizable sugars. *Appl. Environ. Microbiol.* 71, 3060–3067. doi: 10.1128/AEM.71.6.3060-3067.2005
- Couto, N., Schooling, S. R., Dutcher, J. R., and Barber, J. (2015). Proteome profiles of outer membrane vesicles and extracellular matrix of *Pseudomonas aeruginosa* biofilms. *J. Proteome Res.* 14, 4207–4222. doi: 10.1021/acs.jproteome.5b00312
- Daubenspeck, J. M., Liu, R., and Dybvig, K. (2016). Rhamnose links moonlighting proteins to membrane phospholipid in *Mycoplasmas*. *PLoS One* 11:e0162505. doi: 10.1371/journal.pone.0162505
- De Angelis, M., Siragusa, S., Campanella, D., Di Cagno, R., and Gobbetti, M. (2015). Comparative proteomic analysis of biofilm and planktonic cells of *Lactobacillus plantarum* DB200. *Proteomics* 15, 2244–2257. doi: 10.1002/pmic.20140363
- de Vos, W. M. (2015). Microbial biofilms and the human intestinal microbiome. *NPJ Biofilms Microbiomes* 1:15005. doi: 10.1038/npjbiofilms.2015.5
- Doron, S., Snyderman, D. R., and Gorbach, S. L. (2005). *Lactobacillus* GG: bacteriology and clinical applications. *Gastroenterol. Clin. North Am.* 34, 483–498. doi: 10.1016/j.gtc.2005.05.011
- Elias, J. E., and Gygi, S. P. (2007). Target-decoy search strategy for increased confidence in large-scale protein identifications by mass spectrometry. *Nat. Methods* 4, 207–214. doi: 10.1038/nmeth1019
- Espino, E., Koskenniemi, K., Mato-Rodriguez, L., Nyman, T. A., Reunanen, J., Koponen, J., et al. (2015). Uncovering surface-exposed antigens of *Lactobacillus rhamnosus* by cell shaving proteomics and two-dimensional immunoblotting. *J. Proteome Res.* 14, 1010–1024. doi: 10.1021/pr501041a
- Flemming, H. C., and Wingender, J. (2010). The biofilm matrix. *Nat. Rev. Microbiol.* 8, 623–633. doi: 10.1038/nrmicro2415

- Flemming, H. C., Wingender, J., Szewzyk, U., Steinberg, P., Rice, S. A., and Kjelleberg, S. (2016). Biofilms: an emergent form of bacterial life. *Nat. Rev. Microbiol.* 14, 563–575. doi: 10.1038/nrmicro.2016.94
- Folsom, J. P., Richards, L., Pitts, B., Roe, F., Ehrlich, G. D., Parker, A., et al. (2010). Physiology of *Pseudomonas aeruginosa* in biofilms as revealed by transcriptome analysis. *BMC Microbiol.* 10:294. doi: 10.1186/1471-2180-10-294
- Foulston, L., Elsholz, A. K., DeFrancesco, A. S., and Losick, R. (2014). The extracellular matrix of *Staphylococcus aureus* biofilms comprises cytoplasmic proteins that associate with the cell surface in response to decreasing pH. *MBio* 5, e01667–e01614. doi: 10.1128/mBio.01667-14
- Galli, B. D., Baptista, D. P., Cavalheiro, F. G., and Gigante, M. L. (2019). *Lactobacillus rhamnosus* GG improves the sensorial profile of Camembert-type cheese: an approach through flash-profile and CATA. *LWT* 107, 72–78. doi: 10.1016/j.lwt.2019.02.077
- Goldenberg, J. Z., Yap, C., Lytvyn, L., Lo, C. K., Beardsley, J., Mertz, D., et al. (2017). Probiotics for the prevention of *Clostridium difficile*-associated diarrhea in adults and children. *Cochrane Database Syst. Rev.* 12:CD006095. doi: 10.1002/14651858.CD006095
- Graf, A. L., Schäuble, M., Rieckmann, L. M., Hoyer, J., Maaß, S., Lalk, M., et al. (2019). Virulence factors produced by *Staphylococcus aureus* biofilms have a moonlighting function contributing to biofilm integrity. *Mol. Cell. Proteomics* doi: 10.1074/mcp.RA118.001120 [Epub ahead of print].
- Gross, M., Cramton, S. E., Götz, F., and Peschel, A. (2001). Key role of teichoic acid net charge in *Staphylococcus aureus* colonization of artificial surfaces. *Infect. Immun.* 69, 3423–3426. doi: 10.1128/IAI.69.5.3423-3426.2001
- Henderson, B., Fares, M. A., and Martin, A. C. R. (2016). “Biological Consequences of Protein Moonlighting” in *Protein Moonlighting in Biology and Medicine*, eds B. Henderson, M. A. Fares, and A. C. Martin (Hoboken, NJ: John Wiley & Sons, Inc.), 81–141. doi: 10.1002/9781118952108.ch6
- Hoffmann, A., Bukau, B., and Kramer, G. (2010). Structure and function of the molecular chaperone trigger factor. *Biochim. Biophys. Acta* 1803, 650–661. doi: 10.1016/j.bbamcr.2010.01.017
- Holland, I. B., Peherstorfer, S., Kanonenberg, K., Lenders, M., Reimann, S., and Schmitt, L. (2016). Type I protein secretion—deceptively simple yet with a wide range of mechanistic variability across the family. *EcoSal Plus* 7, 1–46. doi: 10.1128/ecosalplus.ESP-0019-2015
- Houston, P., Rowe, S. E., Pozzi, C., Waters, E. M., and O’Gara, J. P. (2011). Essential role for the major autolysin in the fibronectin-binding protein-mediated *Staphylococcus aureus* biofilm phenotype. *Infect. Immun.* 79, 1153–1165. doi: 10.1128/IAI.00364-10
- Ishihama, Y., Oda, Y., Tabata, T., Sato, T., Nagasu, T., Rappsilber, J., et al. (2005). Exponentially modified protein abundance index (emPAI) for estimation of absolute protein amount in proteomics by the number of sequenced peptides per protein. *Mol. Cell. Proteomics* 4, 1265–1272. doi: 10.1074/mcp.m500061-mcp200
- Jakava-Viljanen, M., Avall-Jääskeläinen, S., Messner, P., Sleytr, U. B., and Palva, A. (2002). Isolation of three new surface layer protein genes (*slp*) from *Lactobacillus brevis* ATCC 14869 and characterization of the change in their expression under aerated and anaerobic conditions. *J. Bacteriol.* 184, 6786–6795. doi: 10.1128/JB.184.24.6786-6795.2002
- Jakob, R. P., Koch, J. R., Burmann, B. M., Schmidpeter, P. A., Hunkeler, M., Hiller, S., et al. (2015). Dimeric structure of the bacterial extracellular foldase PrsA. *J. Biol. Chem.* 290, 3278–3292. doi: 10.1074/jbc.M114.622910
- Jiang, Q., Kainulainen, V., Stamatova, I., Korpela, R., and Meurman, J. H. (2018). *Lactobacillus rhamnosus* GG in experimental oral biofilms exposed to different carbohydrate sources. *Caries Res.* 52, 220–229. doi: 10.1159/000479380
- Jiang, Q., Stamatova, I., Kainulainen, V., Korpela, R., and Meurman, J. H. (2016). Interactions between *Lactobacillus rhamnosus* GG and oral micro-organisms in an *in vitro* biofilm model. *BMC Microbiol.* 16:149. doi: 10.1186/s12866-016-0759-7
- Jiang, Q., Stamatova, I., Kari, K., and Meurman, J. H. (2015). Inhibitory activity *in vitro* of probiotic lactobacilli against oral *Candida* under different fermentation conditions. *Benef. Microbes* 6, 361–368. doi: 10.3920/BM2014.0054
- Jones, S. E., and Versalovic, J. (2009). Probiotic *Lactobacillus reuteri* biofilms produce antimicrobial and anti-inflammatory factors. *BMC Microbiol.* 9:35. doi: 10.1186/1471-2180-9-35
- Kainulainen, V., and Korhonen, T. K. (2014). Dancing to another tune—adhesive moonlighting proteins in bacteria. *Biology* 3, 178–204. doi: 10.3390/biology3010178
- Kainulainen, V., Loimaranta, V., Pekkala, A., Edelman, S., Antikainen, J., Kylväjä, R., et al. (2012). Glutamine synthetase and glucose-6-phosphate isomerase are adhesive moonlighting proteins of *Lactobacillus crispatus* released by epithelial cathelicidin LL-37. *J. Bacteriol.* 194, 2509–2519. doi: 10.1128/JB.06704-11
- Kainulainen, V., Reunanen, J., Hiippala, K., Guglielmetti, S., Vesterlund, S., Palva, A., et al. (2013). BopA does not have a major role in the adhesion of *Bifidobacterium bifidum* to intestinal epithelial cells, extracellular matrix proteins, and mucus. *Appl. Environ. Microbiol.* 79, 6989–6997. doi: 10.1128/AEM.01993-13
- Kankainen, M., Paulin, L., Tynkkynen, S., von Ossowski, I., Reunanen, J., Partanen, P., et al. (2009). Comparative genomic analysis of *Lactobacillus rhamnosus* GG reveals pili containing a human-mucus binding protein. *Proc. Natl. Acad. Sci. U.S.A.* 106, 17193–17198. doi: 10.1073/pnas.0908876106
- Klein, M. I., Xiao, J., Lu, B., Delahunty, C. M., Yates, J. R., and Koo, H. (2012). *Streptococcus mutans* protein synthesis during mixed-species biofilm development by high-throughput quantitative proteomics. *PLoS One* 7:e45795. doi: 10.1371/journal.pone.0045795
- Koch, M., Flür, S., Kreutz, C., Ennifar, E., Micura, R., and Polacek, R. (2015). Role of a ribosomal RNA phosphate oxygen during the EF-G-triggered GTP hydrolysis. *Proc. Natl. Acad. Sci. U.S.A.* 112, E2561–E2568. doi: 10.1073/pnas.1505231112
- Kontinen, V. P., and Sarvas, M. (1993). The PrsA lipoprotein is essential for protein secretion in *Bacillus subtilis* and sets a limit for high-level secretion. *Mol. Microbiol.* 8, 727–737. doi: 10.1111/j.1365-2958.1993.tb01616.x
- Krogh, A., Larsson, B., von Heijne, G., and Sonnhammer, E. L. (2001). Predicting transmembrane protein topology with a hidden Markov model: application to complete genomes. *J. Mol. Biol.* 305, 567–580. doi: 10.1006/jmbi.2000.4315
- Lebeer, S., Claes, I., Tytgat, H. L., Verhoeven, T. L., Marien, E., von Ossowski, I., et al. (2012). Functional analysis of *Lactobacillus rhamnosus* GG pili in relation to adhesion and immunomodulatory interactions with intestinal epithelial cells. *Appl. Environ. Microbiol.* 78, 185–193. doi: 10.1128/AEM.06192-11
- Lebeer, S., Claes, I. J., Verhoeven, T. L., Vanderleyden, J., and De Keersmaecker, S. C. (2011a). Exopolysaccharides of *Lactobacillus rhamnosus* GG form a protective shield against innate immune factors in the intestine. *Microb. Biotechnol.* 4, 368–374. doi: 10.1111/j.1751-7915.2010.00199.x
- Lebeer, S., Verhoeven, T. L., Claes, I. J., De Hertogh, G., Vermeire, S., Buyse, J., et al. (2011b). FISH analysis of *Lactobacillus* biofilms in the gastrointestinal tract of different hosts. *Lett. Appl. Microbiol.* 52, 220–226. doi: 10.1111/j.1472-765X.2010.02994.x
- Lebeer, S., De Keersmaecker, S. C., Verhoeven, T. L., Fadda, A. A., Marchal, K., and Vanderleyden, J. (2007a). Functional analysis of *luxS* in the probiotic strain *Lactobacillus rhamnosus* GG reveals a central metabolic role important for growth and biofilm formation. *J. Bacteriol.* 189, 860–871. doi: 10.1128/JB.01394-06
- Lebeer, S., Verhoeven, T. L. A., Velez, M. P., Vanderleyden, J., and De Keersmaecker, S. C. J. (2007b). Impact of environmental and genetic factors on biofilm formation by the probiotic strain *Lactobacillus rhamnosus* GG. *Appl. Environ. Microbiol.* 73, 6768–6775. doi: 10.1128/aem.01393-07
- Lebeer, S., Verhoeven, T. L., Francius, G., Schoofs, G., Lambrechts, I., Dufrene, Y., et al. (2009). Identification of a gene cluster for the biosynthesis of a long, galactose-rich exopolysaccharide in *Lactobacillus rhamnosus* GG and functional analysis of the priming glycosyltransferase. *Appl. Environ. Microbiol.* 75, 3554–3563. doi: 10.1128/AEM.02919-08
- Lee, Y. K., and Puong, K. Y. (2002). Competition for adhesion between probiotics and human gastrointestinal pathogens in the presence of carbohydrate. *Br. J. Nutr.* 1, 101–108. doi: 10.1079/BJN2002635
- Liu, X. D., Xie, L., Wei, Y., Zhou, X., Jia, B., Liu, J., et al. (2014). Abiotic stress resistance, a novel moonlighting function of ribosomal protein RPL44 in the halophilic fungus *Aspergillus glaucus*. *Appl. Environ. Microbiol.* 80, 4294–4300. doi: 10.1128/AEM.00292-14



- Mashruwala, A. A., van de Guchte, A., and Boyd, J. M. (2017). Impaired respiration elicits SrrAB-dependent programmed cell lysis and biofilm formation in *Staphylococcus aureus*. *eLife* 6, e23845. doi: 10.7554/eLife.23845
- Nishiyama, K., Nakamata, K., Ueno, S., Terao, A., Aryantini, N. P., Sujaya, I. N., et al. (2015). Adhesion properties of *Lactobacillus rhamnosus* mucus-binding factor to mucin and extracellular matrix proteins. *Biosci. Biotechnol. Biochem.* 79, 271–279. doi: 10.1080/09168451.2014.972325
- Olson, J. K., Rager, T. M., Navarro, J. B., Mashburn-Warren, L., Goodman, S. D., and Besner, G. E. (2016). Harvesting the benefits of biofilms: a novel probiotic delivery system for the prevention of necrotizing enterocolitis. *J. Pediatr. Surg.* 51, 936–941. doi: 10.1016/j.jpedsurg.2016.02.062
- Poquet, I., Saint, V., Seznec, E., Simoes, N., Bolotin, A., and Gruss, A. (2000). HtrA is the unique surface housekeeping protease in *Lactococcus lactis* and is required for natural protein processing. *Mol. Microbiol.* 35, 1042–1051. doi: 10.1046/j.1365-2958.2000.01757.x
- Quivey, R. G. Jr., Grayhack, E. J., Faustoferri, R. C., Hubbard, C. J., Baldeck, J. D., Wolf, A. S., et al. (2015). Functional profiling in *Streptococcus mutans*: construction and examination of a genomic collection of gene deletion mutants. *Mol. Oral Microbiol.* 30, 474–495. doi: 10.1111/omi.2015.30.issue-6
- Reeves, P. (1993). Evolution of *Salmonella* O antigen variation by interspecific gene transfer on a large scale. *Trends Genet.* 9, 17–22. doi: 10.1016/0168-9525(93)90067-R
- Reichmann, N. T., Cassona, C. P., and Gründling, A. (2013). Revised mechanism of d-alanine incorporation into cell wall polymers in Gram-positive bacteria. *Microbiology* 159(Pt 9), 1868–1877. doi: 10.1099/mic.0.069898-0
- Rice, K. C., Mann, E. E., Endres, J. L., Weiss, E. C., Cassat, J. E., Smeltzer, M. S., et al. (2007). The *cidA* murein hydrolase regulator contributes to DNA release and biofilm development in *Staphylococcus aureus*. *Proc. Natl. Acad. Sci. U.S.A.* 104, 8113–8118. doi: 10.1073/pnas.0610226104
- Rieu, A., Aoudia, N., Jegou, G., Chluba, J., Yousfi, N., Briandet, R., et al. (2014). The biofilm mode of life boosts the anti-inflammatory properties of *Lactobacillus*. *Cell Microbiol.* 16, 1836–1853. doi: 10.1111/cmi.12331
- Sandberg, M., Määttä, A., Peltonen, J., Vuorela, P. M., and Fallarero, A. (2008). Automating a 96-well microtiter plate model for *Staphylococcus aureus* biofilms: an approach to screening of natural antimicrobial compounds. *Int. J. Antimicrob. Agents* 32, 233–240. doi: 10.1016/j.ijantimicag.2008.04.022
- Sanders, M. E., Guarner, F., Guerrant, R., Holt, P. R., Quigley, E. M., Sartor, R. B., et al. (2013). An update on the use and investigation of probiotics in health and disease. *Gut* 62, 787–796. doi: 10.1136/gutjnl-2012-302504
- Santhanalakshmi, J., and Balaji, S. (2001). Binding studies of crystal violet on proteins. *Colloids Surf. A Physicochem. Eng. Asp.* 186, 173–177. doi: 10.1016/S0927-7757(00)00824-4
- Savijoki, K., Lietzén, N., Kankainen, M., Alatossava, T., Koskenniemi, K., Varmanen, P., et al. (2011). Comparative proteome cataloging of *Lactobacillus rhamnosus* strains GG and Lc705. *J. Proteome Res.* 10, 3460–3473. doi: 10.1021/pr2000896
- Siezen, R. J., and Wilson, G. (2010). Probiotics genomics. *Microb. Biotechnol.* 3, 1–9. doi: 10.1111/j.1751-7915.2009.00159.x
- Son, S. H., Park, M. C., and Kim, S. (2014). Extracellular activities of aminoacyl-tRNA synthetases: new mediators for cell-cell communication. *Top. Curr. Chem.* 344, 145–166. doi: 10.1007/128\_2013\_476
- Sonnenburg, E. D., Sonnenburg, J. L., Manchester, J. K., Hansen, E. E., Chiang, H. C., and Gordon, I. (2006). A hybrid two-component system protein of a prominent human gut symbiont couples glycan sensing *in vivo* to carbohydrate metabolism. *Proc. Natl. Acad. Sci. U.S.A.* 103, 8834–8839. doi: 10.1073/pnas.0603249103
- Spatafora, G. A., Sheets, M., June, R., Luyimbazi, D., Howard, K., Hulbert, R., et al. (1999). Regulated expression of the *Streptococcus mutans* *dlt* genes correlates with intracellular polysaccharide accumulation. *J. Bacteriol.* 181, 2363–2372.
- Stoodley, P., Sauer, K., Davies, D. G., and Costerton, J. W. (2002). Biofilms as complex differentiated communities. *Annu. Rev. Microbiol.* 56, 187–209. doi: 10.1146/annurev.micro.56.012302.160705
- Stothard, P. (2000). The sequence manipulation suite: javascript programs for analyzing and formatting protein and DNA sequences. *Biotechniques* 28, 1102–1104. doi: 10.2144/00286ir01
- Townsend, G. E. II, Han, W., Schwalm, N. D. III, Raghavan, V., Barry, N. A., Goodman, A. L., et al. (2019). Dietary sugar silences a colonization factor in a mammalian gut symbiont. *Proc. Nat. Acad. Sci. U.S.A.* 116, 233–238. doi: 10.1073/pnas.1813780115
- Trent, M. S., Stead, C. M., Tran, A. X., and Hankins, J. V. (2006). Diversity of endotoxin and its impact on pathogenesis. *J. Endotoxin Res.* 12, 205–223. doi: 10.1179/096805106X118825
- Tytgat, H. L., Schoofs, G., Vanderleyden, J., Van Damme, E. J., Wattiez, R., Lebeer, S., et al. (2016). Systematic exploration of the glycoproteome of the beneficial gut isolate *Lactobacillus rhamnosus* GG. *J. Mol. Microbiol. Biotechnol.* 26, 345–358. doi: 10.1159/000447091
- Varmanen, P., Vesanto, E., Steele, J. L., and Palva, A. (1994). Characterization and expression of the pepN gene encoding a general aminopeptidase from *Lactobacillus helveticus*. *FEMS Microbiol. Lett.* 124, 315–320. doi: 10.1016/0378-1097(94)00447-1
- Velez, M. P., Petrova, M. I., Lebeer, S., Verhoeven, T. L., Claes, I., and Lambrichts, I. (2010). Characterization of MAbA, a modulator of *Lactobacillus rhamnosus* GG adhesion and biofilm formation. *FEMS Immunol. Med. Microbiol.* 59, 386–398. doi: 10.1111/j.1574-695X.2010.00680.x
- Vesterlund, S., Karp, M., Salminen, S., and Ouwehand, A. C. (2006). *Staphylococcus aureus* adheres to human intestinal mucus but can be displaced by certain lactic acid bacteria. *Microbiology* 152, 1819–1826. doi: 10.1099/mic.0.28522-0
- von Ossowski, I., Satokari, R., Reunanen, J., Lebeer, S., De Keersmaecker, S. C. J., Vanderleyden, J., et al. (2011). Functional characterization of a mucus-specific LPXTG surface adhesin from probiotic *Lactobacillus rhamnosus* GG. *Appl. Environ. Microbiol.* 77, 4465–4472. doi: 10.1128/AEM.02497-10
- Wang, W., and Jeffery, C. J. (2016). An analysis of surface proteomics results reveals novel candidates for intracellular/surface moonlighting proteins in bacteria. *Mol. Biosyst.* 12, 1420–1431. doi: 10.1039/c5mb00550g
- Wei, R., Wang, J., Jia, E., Chen, T., Ni, Y., and Jia, W. (2018a). GSimp: a gibbs samples based left-censored missing value imputation approach for metabolomics studies. *PLoS Comput. Biol.* 14:e1005973. doi: 10.1371/journal.pcbi.1005973
- Wei, R., Wang, J., Su, M., Jia, E., Chen, S., Chen, T., et al. (2018b). Missing value imputation approach for mass spectrometry-based metabolomics data. *Sci. Rep.* 8:663. doi: 10.1038/s41598-017-19120-0
- Welch, K., Yanling, C., and Strømme, M. (2012). A method for quantitative determination of biofilm viability. *J. Funct. Biomater.* 3, 3418–3431.
- Yu, Y., Wagner, J. R., Laird, M. R., Melli, G., Rey, S., Lo, R., et al. (2010). PSORTb 3.0: improved protein subcellular localization prediction with refined localization subcategories and predictive capabilities for all prokaryotes. *Bioinformatics* 26, 1608–1615. doi: 10.1093/bioinformatics/btq249

**Conflict of Interest Statement:** The authors declare that the research was conducted in the absence of any commercial or financial relationships that could be construed as a potential conflict of interest.

Copyright © 2019 Savijoki, Nyman, Kainulainen, Miettinen, Siljamäki, Fallarero, Sandholm, Satokari and Varmanen. This is an open-access article distributed under the terms of the Creative Commons Attribution License (CC BY). The use, distribution or reproduction in other forums is permitted, provided the original author(s) and the copyright owner(s) are credited and that the original publication in this journal is cited, in accordance with accepted academic practice. No use, distribution or reproduction is permitted which does not comply with these terms.